Negative Cooperativity in the Binding of Nucleotides to *Escherichia coli* Replicative Helicase DnaB Protein. Interactions with Fluorescent Nucleotide Analogs†

Wlodzimierz Bujalowski* and Malgorzata Maria Klonowska‡

Department of Human Biological Chemistry and Genetics, The University of Texas Medical Branch Galveston, Galveston, Texas 77555-0653

Received January 21, 1993; Revised Manuscript Received March 4, 1993

ABSTRACT: The interactions of nucleotides with *Escherichia coli* replicative helicase DnaB protein have been systematically studied using fluorescent nucleotide analogs, 2′(3′)-*O*-(2,4,6-trinitrophenyl)adenosine 5′-triphosphate (TNP-ATP), 2′(3′)-*O*-(2,4,6-trinitrophenyl)adenosine 5′-diphosphate (TNP-ADP), 2′(3′)-*O*-(2,4,6-trinitrophenyl)adenosine 5′-monophosphate (TNP-AMP), 3′-*O*-(*N*-methylantraniloyl) 5′-diphosphate (MANT-ADP), and 1,N^6-ethenoadenosine diphosphate (εADP). The binding of the analogs is accompanied by strong quenching of the protein fluorescence; 0.76 ± 0.05, 0.76 ± 0.05, 0.58 ± 0.05, and 0.53 ± 0.5 for TNP-ATP, TNP-ADP, MANT-ADP, and εADP, respectively. A thermodynamically rigorous method has been applied to obtain all binding parameters from fluorescence titration curves independent of the assumption of strict proportionality between the observed quenching of the protein fluorescence and the degree of nucleotide binding. An exact representation of the observed fluorescence quenching, as a function of the nucleotide binding, is introduced through an empirical function which enables analysis of single binding isotherms without the necessity of determining all quenching constants for different binding sites. Using this method, we determined that, at saturation, the DnaB hexamer binds six molecules of TNP-ATP, TNP-ADP, MANT-ADP, and εADP, and that there is strong heterogeneity among nucleotide binding sites. The binding isotherms are biphasic. Three molecules of nucleotide are bound in the first high-affinity binding phase, and the subsequent three molecules are bound in the second low-affinity binding phase. The separation of the two binding steps is even more pronounced at higher temperatures. The change of the monitored fluorescence is sequential. The binding of the first nucleotide causes the largest quenching of the protein fluorescence with subsequent nucleotide binding inducing progressively less quenching. The simplest explanation of this behavior is that there is a negative cooperativity among nucleotide binding sites on a DnaB hexamer. The negative cooperativity is an intrinsic property of the DnaB helicase, since it is observed in the binding of nucleotide analogs which are different in type and location of the modifying group. A statistical thermodynamic model is proposed, the hexagon, which provides an excellent description of the binding process using only two interaction parameters, intrinsic binding constant K and cooperativity parameter σ. The data suggest an important role of the phosphate groups in binding and in recognition of nucleotides by the DnaB helicase.

The DnaB protein is a crucial replication protein in *Escherichia coli* (Kornberg & Baker, 1992). The protein is involved both in initiation and elongation stages of DNA replication and plays a key role in the replication of bacterial chromosomal, phage, and plasmid DNA (McMacken et al., 1977; Ueda et al., 1978; Kaguni et al., 1982; Matson & Kaiser-Rogers, 1990). Recent studies show that the protein is the *E. coli* primary replicative helicase, i.e., the factor responsible for the unwinding of the DNA duplex in front of the replication fork (LeBowitz & McMacken, 1986; Baker et al., 1987). In its role as a "mobile replication promoter" DnaB protein binds to ssDNA and produces a unique secondary structure which is then recognized by the primase (Arai & Kornberg, 1981b).

Studies *in vitro* demonstrate that DnaB protein displays multiple activities: (1) binding of rNTPs (particularly ATP) and dNTPs (Arai & Kornberg, 1981a–c; Arai et al., 1981a; Reha-Krantz & Hurwitz, 1978b); (2) ATPase and ribonucleotide triphosphatase activities (Arai & Kornberg, 1981a–c; Reha-Krantz & Hurwitz, 1978b; Lebowitz & McMacken, 1986); (3) binding to ss- and dsDNA (Arai & Kornberg, 1981a,b; Reha-Krantz & Hurwitz, 1978b; Lebowitz & McMacken, 1986); (4) interactions with DnaC protein (Kobori & Kornberg, 1982a–c; Wahle et al., 1989; Allen & Kornberg, 1991), primase (DnaG protein) (Arai & Kornberg, 1981b; Lebowitz & McMacken, 1986), phage λ-encoded P protein (Wickner, 1978; Mallory et al., 1990), and phage P1-encoded Ban protein (Lanka et al., 1978); (5) stimulation of its helicase activity by the single strand binding (SSB) protein (LeBowitz & McMacken, 1986). These multiple activities reflect interactions of DnaB with different ingredients in the primosome and in the protein–nucleic acid complexes formed at the origins of bacterial and phage DNA replication.

The DnaB protein was originally isolated on the basis of its requirement for *in vitro* φX174 phage replication (Wickner et al., 1973; Schekman et al., 1974, 1975; McMacken et al., 1977; Ueda et al., 1978). The gene encoding the DnaB protein has been cloned. Its sequence, and that of the encoded protein, has been determined (Nakayama et al., 1984a,b). The native protein is a hexamer composed of six identical subunits with a monomeric molecular weight of 52 265 (Nakayama et al.,

† This work was supported by NIH Grant R01 GM-46679 (to W.B.). Support from the John Sealy Foundation is also acknowledged.

* Correspondence should be addressed to this author.

‡ On leave from the Laboratory of Physical Chemistry, Drug Science Institute, Department of Pharmacy, Warsaw Medical School, Banacha 1, Warsaw, Poland.

0006-2960/93/0432-5888$04.00/0

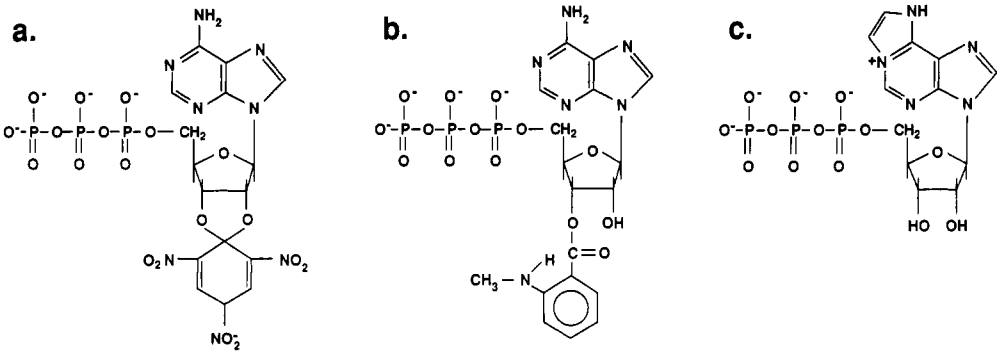

FIGURE 1: Structure of TNP-ATP, MANT-ATP, and εATP (Hiratsuka & Uchida, 1973; Hiratsuka, 1983; Secrist et al., 1972).

1984a,b; Arai et al., 1981a; Reha-Krantz & Hurwitz, 1978a).

The functions of the DnaB protein *in vivo* are related to its ability to interact with ss- and dsDNA under ATP control. The binding or binding and hydrolysis of ATP regulate enzyme activity and affinity toward nucleic acids and other components of the replication apparatus (Arai & Kornberg, 1981a–c; Reha-Krantz & Hurwitz, 1978b; LeBowitz & McMacken, 1986). Hydrolysis of ATP is not necessary for binding of DnaB protein to ssDNA. In the presence of the nonhydrolyzable ATP analogs ATPγS[1] and App(NH)p, the affinity of the enzyme to ssDNA is even higher. In contrast, ADP and dNTPs have been found to strongly inhibit DnaB binding to ssDNA (Arai & Kornberg, 1981b). ATP is also required for the formation of the specific structure in the DnaB–ssDNA complex, which is a recognition signal for primase and is inhibited in the presence of ADP (Arai & Kornberg, 1981b). These results suggest that ATP acts as a very specific positive allosteric effector inducing a conformational change in the protein and increasing its affinity for single stranded nucleic acids. On the other hand, ADP and dNTPs act as negative effectors for the interaction of DnaB protein with ssDNA.

Helicases are the enzymes which perform the actual unwinding of the DNA duplex at the replication fork (Matson & Kaiser-Rogers, 1990). The unwinding of duplex DNA by DnaB protein requires hydrolyzable ribonucleoside triphosphates, with ATP being the most efficient. Neither nonhydrolyzable analogs nor dNTPs support the reaction (LeBowitz & McMacken, 1986).

It is clear that understanding the nucleotide interactions with DnaB protein and its regulatory role is a key element in our understanding of the different activities of this enzyme. Although the importance of the control and regulation of the DnaB protein functions by nucleoside phosphates has been recognized, the mechanism and the nature of this control remains obscure, particularly at the molecular level.

There is a significant controversy concerning the stoichiometry of the DnaB–nucleotide complex. Six nucleotide binding sites have been identified on the DnaB hexamer by equilibrium gel filtration and filter binding assays at 0 °C (Arai & Kornberg, 1981b). It has been suggested that each DnaB promoter has one ATP binding site. No heterogeneity among nucleotide binding sites has been observed. On the other hand, recent studies with the ATP fluorescent analogs TNP-ATP and TNP-ADP have indicated the existence of only three binding sites on the hexamer (Biswas et al., 1986; Biswas & Biswas, 1987). No heterogeneity among these binding sites has been observed.

Fluorescent nucleotide analogs are extremely useful in studying the mechanism of enzymatic activity of different triphosphatases (Secrist et al., 1972; Hiratsuka & Uchida, 1973; Moczydlowski & Fortes, 1981a,b; Bruist & Hammes, 1982; Perkins et al., 1984; Cheung et al., 1985). Applications of the analogs enable not only the stoichiometry and the mechanism of the complex formation to be determined but also the existence of intermediates in the enzyme catalysis, as well as the location and the nature of the binding sites.

In this paper we systematically investigate the interactions of adenosine nucleotide fluorescent analogs TNP-ATP, TNP-ADP, TNP-AMP, MANT-ADP, and εADP with the DnaB hexamer. These analogs differ by the type and location of the modifying groups. In the case of TNP and MANT derivatives, the modifications are located on the ribose, while the etheno derivative is modified on the adenine residue. The structural formulas of the ATP derivatives of the studied fluorescent analogs are shown in Figure 1. We found that the binding of TNP, MANT, and etheno analogs to the enzyme is accompanied by strong quenching of the protein tryptophan fluorescence, which is mainly due to fluorescence energy transfer from tryptophans to the nucleotide (Bujalowski and Klonowska, manuscript in preparation). Therefore, instead of studying the enhancement of the fluorescence of the nucleotide analog, as it is usually performed, we followed the binding by monitoring the signal from the macromolecule (protein fluorescence). This approach made the measurements more reliable and greatly simplified the analysis (Bujalowski & Lohman, 1987; Halfman & Nishida, 1972; Lohman & Bujalowski, 1991). In these studies we applied a general method which enables the determination of the ligand–macromolecule stoichiometry from spectroscopic measurements without making any assumptions about the relationship between the number of the bound nucleotides and the signal from the macromolecule. This results in absolute stoichiometries and thermodynamically rigorous binding isotherms.

We present direct evidence that there are six nucleotide binding sites on the DnaB hexamer which differ dramatically in affinity. This is particularly pronounced at higher temperatures. The binding process is biphasic, and we suggest that the observed heterogeneity reflects negative cooperativity between binding sites and that it is an intrinsic property of the DnaB hexamer. To describe the biphasic behavior of the binding isotherm, we propose a statistical thermodynamic model that quantitatively describes the binding process and enables us to dissect the contribution of intrinsic nucleotide affinity from negative cooperative interactions.

[1] Abbreviations: ATPγS, adenosine 5′-*O*-(3-thiotriphosphate); App(NH)p, β,γ-imodoadenosine 5′-triphosphate; TNP-ATP, 2′(3′)-*O*-(2,4,6-trinitrophenyl)adenosine 5′-triphosphate; TNP-ADP, 2′(3′)-*O*-(2,4,6-trinitrophenyl)adenosine 5′-diphosphate; TNP-AMP, 2′(3′)-*O*-(2,4,6-trinitrophenyl)adenosine 5′-monophosphate; εADP, 1,N^6-ethenoadenosine diphosphate; MANT-ADP, 3′-*O*-(*N*-methylantraniloyl) 5′-diphosphate; SSB, *E. coli* single strand binding protein; Tris, tris(hydroxymethyl)-aminomethane.

MATERIALS AND METHODS

Reagents and Buffers. All chemicals were reagent grade. All solutions were made with distilled and deionized 18 MΩ (Milli-Q) water. The standard buffer (T2) is 50 mM Tris adjusted to pH 8.1 at appropriate temperatures with HCl, 5 mM $MgCl_2$, and 10% glycerol. The temperatures and the concentrations of NaCl in the buffer are indicated in the text.

Nucleotides. TNP-ATP, TNP-ADP, TNP-AMP, and MANT-ADP were from Molecular Probes (Eugene, OR). The nucleotides were additionally purified as described by Hiratsuka and Uchida (1973). ϵADP was from Sigma and was used without further purification. All nucleotides used in the binding studies were >95% pure as judged by TLC on silica.

DnaB Protein. The *E. coli* DnaB protein was purified from RLM1038 overproducing strain generously provided by Dr. Roger McMacken (Johns Hopkins University). The protein was purified using a slightly modified Arai–Kornberg procedure (Arai et al., 1981a). The cells were first disrupted by temperature shock, followed by the addition of 0.03% (w/v) sodium deoxycholate. ATP was omitted in the isolation buffers; no effect on protein stability and activity was found when ATP was either included or omitted in the isolation procedure. The protein was >97% pure as judged by SDS–polyacrylamide gel electrophoresis with Coomasie Brilliant Blue staining. The concentration of the protein was determined spectrophotometrically using an extinction coefficient $\epsilon_{280} = 1.85 \times 10^5$ cm^{-1} M^{-1} (hexamer) (Bujalowski and Klonowska, manuscript in preparation).

Fluorescence Measurements. All titrations of DnaB protein with fluorescent nucleotide analogs were performed using the SLM 48000S lifetime spectrofluorometer. In order to avoid possible artifacts due to the fluorescence anisotropy of the sample, polarizers were placed in excitation and emission channels and set at 90° and 55° (magic angle), respectively. The binding was followed by monitoring the quenching of the protein tryptophan fluorescence (λ_{ex} = 300 nm; λ_{em} = 345 nm). All titration points were corrected for dilution and inner filter effects using the following formula (Parker, 1968; Lakowicz, 1983):

$$F_{icor} = (F_i - B_i)(V_i/V_o)10^{0.5b(A_{i\lambda ex}+A_{i\lambda em})} \quad (1)$$

where F_{icor} is the corrected value of the fluorescence intensity at a given point of titration i, F_i is the experimentally measured fluorescence intensity, B_i is the background, V_i is the volume of the sample at a given titration point, V_o is the initial volume of the sample, b is the total length of the optical path in the cuvette expressed in centimeters, and $A_{i\lambda ex}$ and $A_{i\lambda em}$ are the absorbances of the sample at excitation and emission wavelengths, respectively. The temperature of the sample was controlled to ±0.1 °C. Nonlinear least-squares fits of binding isotherms and computer simulations were performed using KaleidaGraph software (Synergy Software PA).

Determination of Rigorous Thermodynamic Binding Isotherms. In the studies described in this work, we measured the binding of nucleotides to DnaB protein by following the quenching of the protein fluorescence. To obtain true thermodynamic binding parameters, it was necessary to determine the relationship between the observed DnaB fluorescence quenching Q_{obsd} and the average degree of binding of nucleotides per DnaB hexamer, $\sum\nu_i$. The following general procedure was used to obtain absolute estimates of $\sum\nu_i$ and the free nucleotide concentration N_f. The method is based on the fact that, if the binding of a ligand (nucleotide) to the macromolecule (DnaB) is accompanied by a change of the physicochemical property of the macromolecule, then the intensive property of the macromolecule (e.g., molar protein fluorescence, absorption) is a unique function of the chemical potential of the free ligand in solution (Bujalowski & Lohman, 1987; Halfman & Nishida, 1972). In general, there are i sites for binding of nucleotides per DnaB hexamer. In this case, experimentally observed Q_{obsd} is functionally related to $\sum\nu_i$ by

$$Q_{obsd} = \sum \nu_i Q_{imax} \quad (2)$$

where Q_{imax} is the maximum quenching of the DnaB protein fluorescence with the nucleotide bound to site i. It should be noted that Q_{imax} is the molecular property of the binding site for a given macromolecule–ligand system and it is a constant, independent of macromolecule or ligand concentration. Thus, Q_{obsd} is simply a degree of binding $\sum\nu_i$ weighted by the contributions to the overall quenching from different binding sites associated with the nucleotide. Therefore, for the same value of Q_{obsd} obtained at two different total protein concentrations M_{T1} and M_{T2}, the degree of binding $\sum\nu_i$ and the free nucleotide concentration N_f must be the same. The value of $\sum\nu_i$ and N_f is then related to the total protein concentrations M_{T1} and M_{T2} and total nucleotide concentrations N_{T1} and N_{T2}, at which the same Q_{obsd} is obtained, by the formula (Bujalowski & Lohman, 1989a)

$$\sum \nu_i = (N_{T2} - N_{T1})/(M_{T2} - M_{T1}) \quad (3)$$

$$N_f = M_{Tx} - \sum \nu_i (M_{Tx}) \quad (4)$$

where x = 1 or 2. Thus, the absolute stoichiometry of the ligand–macromolecule complex can be obtained, which allows us to correlate of $\sum\nu_i$ with Q_{obsd}. This procedure is particularly important in the case of DnaB–nucleotide binding, because of the nonlinear dependence of the extent of fluorescence quenching upon the degree of binding (see Results). If all optical (Q_{imax}) and interaction parameters (intrinsic binding constants, cooperativity parameters) are known, then eq 2 is an analytical formula which describes the dependence of the intensive property of the macromolecule as a function of the free ligand concentration.

It should be noted that it is necessary to apply the procedure to the binding system to establish the relationship between Q_{obsd} and $\sum\nu_i$ and to verify that it is true over the range of studied solution conditions. The obtained relationship can then be used to determine true binding parameters from a single titration curve by simply converting it to an absolute binding isotherm, i.e., a plot of the average degree of binding as a function of the concentratin of ligand (nucleotides).

In some simple cases, all optical and interaction parameters in the analytical formula relating Q_{obsd} to molecular parameters Q_{imax} can be found (Bujalowski & Lohman, 1989a,b). However, as we show below, this is not necessary, and in the case of DnaB protein, which has six nucleotide binding sites and possibly multiple Q_{imax} for a given number of bound nucleotide molecules, practically impossible. For instance, in the case of the hexagon model for DnaB–nucleotide system, there are at least 10 optical parameters (see below). In this case we applied the following approach, which can be used for any ligand–macromolecule systems, where the determination of all optical constants in an analytical equation is practically impossible. An empirical function, usually polynomial, was found, which exactly related the experimentally determined dependence of the average quenching Q_{obsd} to $\sum\nu_i$. We achieved this by using a nonlinear least-squares fit of Q_{obsd} as a function of $\sum\nu_i$. In the case of DnaB–nucleotide interactions, a

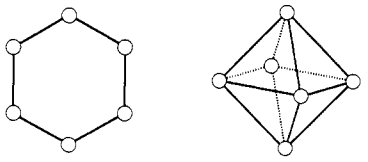

FIGURE 2: Cartoon representing the hexagon (a) and octahedron (b) models of the DnaB protein hexamer. The circles represent subunits and the lines connecting each subunit with its neighbors symbolize the number of possible cooperative interactions in each model (two in hexagon and four in octahedron).

minimum third degree polynomial was necessary to describe this function as defined by

$$Q_{obsd} = a(\sum \nu_i) + b(\sum \nu_i)^2 + c(\sum \nu_i)^3 \quad (5)$$

where a, b, and c are fitting constants. This function was then used to generate a theoretical isotherm for a binding model and to extract true binding parameters from the experimentally obtained single isotherm. To generate the theoretical isotherm, the value of the degree of binding $\sum \nu_i$ was calculated, for a given free nucleotide concentration and initial estimates of intrinsic binding constant K and cooperativity parameter σ, using eq 9. The obtained $\sum \nu_i$ was then introduced into eq 5, and the fluoresence quenching corresponding to this value of the degree of binding was calculated. These calculations were performed for the whole titration curve. Optimization of the binding parameters K and σ was obtained using nonlinear least-squares fit (see below).

THEORY

Statistical Thermodynamic Model for the Nucleotide Binding to the DnaB Protein Hexamer with Cooperative Interactions among Binding Sites. The absolute thermodynamic isotherms determined in this work, using the general analysis described under Materials and Methods, show that binding of nucleotides to the DnaB hexamer is characterized by the strong decrease of the affinity with the increase of the degree of binding. The simplest explanation for this behavior is that the DnaB hexamer exhibits negative cooperativity between binding sites. The other possibility is that the DnaB hexamer possesses at least two independent classes of binding sites with different affinities. We favor the former explanation of negative cooperativity for the reasons presented under Results and Discussion.

Two simple models that can incorporate negative cooperativity among six ligand binding sites on a hexamer are depicted in Figure 2a,b (Hill, 1985). Both models use only two parameters to describe the binding: the intrinsic binding constant K and cooperativity parameter σ. They differ from each other in the "density" of the cooperative interactions among binding sites. The model in Figure 2a is a hexagon of six binding sites, and the first ligand can bind to any of six initially equivalent binding sites with intrinsic binding constant K. The cooperative interactions are limited to only two neighboring sites. In the octahedrion model (Figure 2b), nucleotides can initially bind to any binding site with intrinsic binding constant K. However, the cooperative interactions may occur among four neighboring sites. As a result, the "density" of interactions is higher in the octahedron than in the hexagon. If we assign the quantity $x = KL$, where L is the free ligand concentration, then the partition functions for hexagon Z_H and octahedron model Z_O are described by

$$Z_H = 1 + 6x + 3(3 + 2\sigma)x^2 + 2(1 + 6\sigma + 3\sigma^2)x^3 + 3(3\sigma^2 + 2\sigma^3)x^4 + 6\sigma^4x^5 + \sigma^6x^6 \quad (6)$$

$$Z_O = 1 + 6x + 3(4\sigma + 1)x^2 + 4(2\sigma^3 + 3\sigma^2)x^3 + 3(\sigma^4 + 4\sigma^5)x^4 + 6\sigma^8x^5 + \sigma^{12}x^6 \quad (7)$$

The average degree of binding $\sum \nu_i$ is defined by the standard statistical thermodynamic formula (Hill, 1985)

$$\sum \nu_i = \partial \ln Z / \partial \ln L \quad (8)$$

and the expressions for the average degree of binding for hexagon and octahedron models are given by

$$(\sum \nu_i)_H = [6x + 6(3 + 2\sigma)x^2 + 6(1 + 6\sigma + 3\sigma^2)x^3 + 12(3\sigma^2 + 2\sigma^3)x^4 + 30\sigma^4x^5 + 6\sigma^6x^6]/Z_H \quad (9)$$

$$(\sum \nu_i)_O = [6x + 6(4\sigma + 1)x^2 + 12(2\sigma^3 + 3\sigma^2)x^3 + 12(\sigma^4 + 4\sigma^5)x^4 + 30\sigma^8x^5 + 6\sigma^{12}x^6]/Z_O \quad (10)$$

It should be stressed that geometrical terms used to describe the two models serve exclusively to describe the density of the cooperative interactions among binding sites and do not necessarily indicate structural features of the DnaB protein hexamer (Hill, 1985).

Inspection of eqs 6 and 7 reveals a significant qualitative difference between these two models which can be used to distinguish between them. In the case of the hexagon model with three ligands bound to the hexamer, there is a configuration which does not result in any cooperative interactions, i.e., three ligands can bind in an independent manner. In the octahedron model, all configurations of the complex with three ligands bound result in cooperative interactions. This difference has a profound effect on the shape of the binding isotherm. Theoretical binding isotherms for these two models for different values of the cooperativity parameter σ are shown in Figure 3a,b. Clearly, there is no qualitative difference between the two models for $\sigma = 1$. However, as the value of σ decreases, the binding isotherm for the hexagon model splits into two distinct binding steps with three ligands binding in the first step (first plateau) and the next three ligands binding in the second step. The behavior of the octahedron model is different. At $\sigma < 1$ the whole binding isothrm shifts toward a higher ligand concentration range, but without any separation into two different binding steps. At a very low value of σ the isotherm splits into three binding steps with two ligand molecules binding in each step.

The DnaB hexamer with a given number of nucleotide molecules bound can exist in multiple configurations, e.g., a hexagon model the hexamer with three ligands bound has 20 possible configurations (see eq 6). Although some of these configurations are physically indistinguishable, resulting from simple statistical effects of binding three molecules to initially independent six sites, there are configurations which differ by the number of cooperative interactions, and they may also differ by the values of the individual molecular quenching constants $Q_{i\max}$. Equation 11 describes the minimum analytical relationship between the observed experimental quenching Q_{obsd}, the individual quenching parameters $Q_{i\max}$, and interaction parameters K and σ, for the hexagon model:

$$Q_{obsd} = [6\Delta Q_1 x + 6(3\Delta Q_{2_1} + 2\sigma\Delta Q_{2_2})x^2 + 6(\Delta Q_{3_1} + 6\sigma\Delta Q_{3_2} + 3\sigma^2\Delta Q_{3_3})x^3 + 12(3\sigma^2\Delta Q_{4_1} + 2\sigma^3\Delta Q_{4_2})x^4 + 30\sigma^4\Delta Q_5x^5 + 6\sigma^6\Delta Q_6x^6]/Z_H \quad (11)$$

For clarity, subscript "max" has been omitted at individual molecular quenching constants $Q_{i\max}$ in eq 11. Equation 11 contains 12 independent parameters, two interaction and 10 optical parameters. For instance, there are three physically

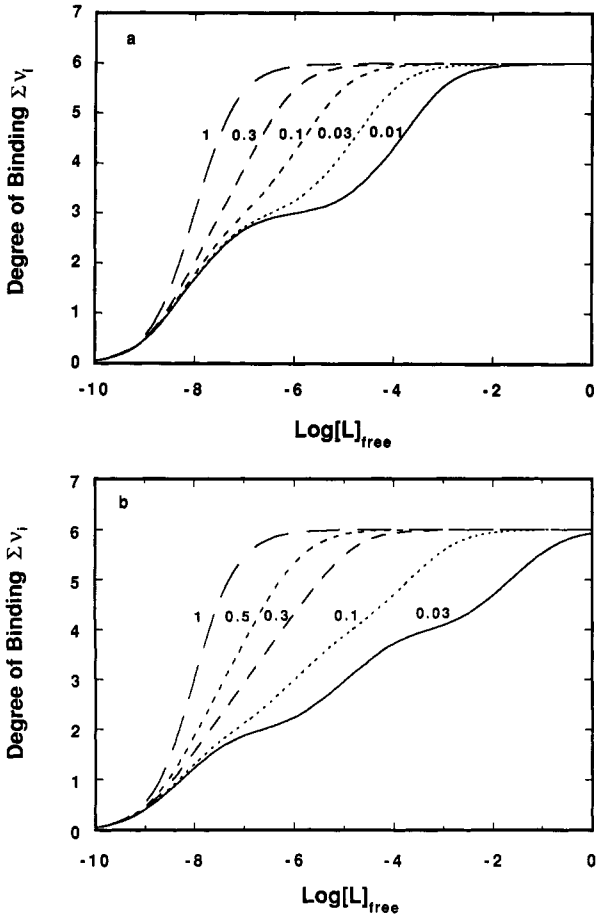

FIGURE 3: Computer simulation of the dependence of the average number of ligand molecules bound per hexamer, $\Sigma\nu_i$, upon the free ligand concentration L_f. (a) Hexagon; (b) Octahedron. The binding isotherms were generated using eqs 9 and 10 in the text, for the different values of the negative cooperativity parameter σ, as indicated in the figure. The value of the intrinsic binding constant K was selected to be 10^8 M^{-1}.

distinguishable configurations of the hexamer with three ligands bound which have different densities of the cooperative interactions; therefore, there are three possible different molecular quenching constants, ΔQ_{3_1}, ΔQ_{3_2}, and ΔQ_{3_3}, characterizing each of these configurations.

In order to apply eq 11 to obtain interaction parameters K and σ from a single binding isotherm, all 10 optical constants, Q_i, must be known. The problem of finding all optical parameters can be avoided by using an empirical function (eq 5) relating the observed quenching to the average degree of binding, as described under Materials and Methods. It should be pointed out that, at the saturating concentration of the ligand, the observed experimental maximum quenching is $Q_{obsd} = \Delta Q_6$. On the other hand, at a very low ligand concentration eq 11 reduces to

$$Q_{obsd} = 6\Delta Q_1 x/(1 + x) \qquad (12)$$

Introducing $x = KL$ and transforming eq 12, one obtains

$$1/Q_{obsd} = (1/6\Delta Q_1 K)(1/L) + 1/6\Delta Q_1 \qquad (13)$$

Plotting $1/Q_{obsd}$ as a function of free ligand concentration L gives a straight line with intercept $1/6\Delta Q_1$ and the slope $1/6\Delta Q_1 K$, providing an independent estimation of intrinsic binding constant K and the molecular quenching constant ΔQ_1. Equation 13 is particularly useful in determining the intrinsic binding constant in the cases where, due to the low affinity, the application of the general method described under

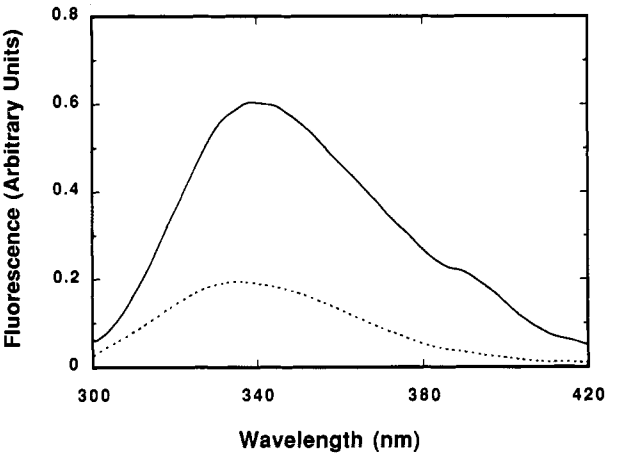

FIGURE 4: Corrected fluorescence emission spectra of the DnaB protein in buffer T2 + 20 mM NaCl (pH 8.1, 10 °C) in the absence (—) and the presence (- - -) of 3×10^{-5} M TNP-ATP; λ_{ex} = 285 nm.

Materials and Methods is difficult, or even impossible (see Results). It should also be pointed out that eqs 12 and 13 can be derived from the general Adair binding equation (Hill, 1985). Therefore these expressions are independent of any particular models, valid in the limit of low affinity and low degree of saturation, and provide an estimation of the intrinsic binding constant for the first binding site.

RESULTS

Absolute Stoichiometries of Nucleotide–DnaB Protein Complexes. In the presence of ssDNA, DnaB protein can hydrolyze TNP-ATP at 30 °C, but, with a velocity of ~100 lower than ATP (Biswas et al., 1986). Without ssDNA, and at a lower temperature (10 °C), the hydrolysis is even slower and negligible on the time scale of the binding experiments performed in this work (Bujalowski and Klonowska, unpublished results).

We found that binding of TNP-ATP to DnaB protein is accompanied by a strong quenching of the protein fluorescence. Corrected fluorescence emission spectra of DnaB protein in buffer T2 + 20 mM NaCl (pH 8.1, 10 °C), in the absence and in the presence of close to saturating concentration (3×10^{-5} M) of TNP-ATP, are shown in Figure 4. Addition of TNP-ATP to the solution causes a strong decrease of protein fluorescence. Also, there is a slight blue-shift of the spectrum with the maximum at λ = 337 nm compared to λ = 341 nm for free protein.

Fluorescence titrations of the DnaB protein with TNP-ATP, at two different protein concentrations, in buffer T2 + 20 mM NaCl, pH 8.1 (10 °C), are shown in Figure 5. The maximum quenching of the protein fluorescence at saturation is 0.76 ± 0.05. The selected protein concentrations differ by factor ~6 giving a good separation of two binding isotherms up to the quenching value of ~0.70. Inspection of the isotherms in Figure 5, particularly at low protein concentration, where the concentration of bound TNP-ATP is small compared to $[TNP\text{-}ATP]_{total}$, shows biphasic character of the binding process. The first higher affinity binding phase is characterized by a large change of the protein fluorescence (quenching up to ~0.55). The second lower affinity binding phase is characterized by a much smaller fluorescence change (quenching up to ~0.23). Using the titrations presented in Figure 5, the absolute stoichiometry of TNP-ATP binding per DnaB hexamer can be calculated using the approach described under Materials and Methods. The correlation between the quenching of the protein fluorescence from 0 to 0.7 and the number

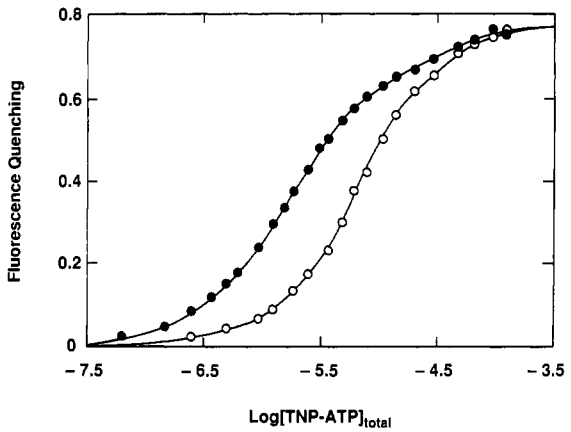

FIGURE 5: Fluorescence titration of the DnaB hexamer with TNP-ATP monitored by the quenching of the intrinsic protein fluorescence in buffer T2 + 20 mM NaCl (pH 8.1, 10 °C) at two different concentrations of the DnaB hexamer: (●) 5.38×10^{-7} M; (○) 3.17×10^{-6} M. Solid lines are added to separate the two data sets and have no theoretical basis.

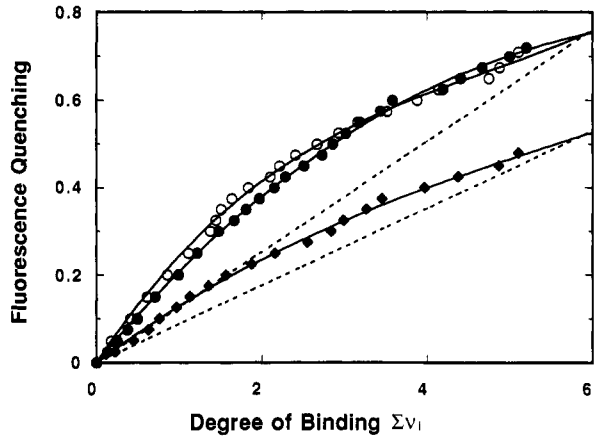

FIGURE 6: Dependence of the quenching of the DnaB protein fluorescence upon the average number of nucleotide molecules bound per DnaB hexamer in buffer T2 + 20 mM NaCl (pH 8.1, 10 °C); (○) TNP-ATP; (●) TNP-ADP; (◆) εADP. The average number of the nucleotides bound, at a particular value of the fluorescence quenching, has been determined from two titrations shown in Figures 5, 7, and 8 for TNP-ATP, TNP-ADP, and εADP, respectively, using eqs 3 and 4 in the text. The dashed line represents the theoretical situation when the strict proportionality between the degree of nucleotide binding and the quenching of the DnaB protein fluorescence existed. Solid lines are generated using the values of parameters (see text) obtained from nonlinear least-squares fits based third degree polynomials described by eq 5.

of TNP-ATP molecules bound per DnaB hexamer from 0 to 5.2 is presented in Figure 6 (open circles). Extrapolation to the maximum quenching $Q_{max} = 0.76$ shows that, at saturation, DnaB protein hexamer binds six molecules of TNP-ATP. The largest change, up to $\sim 0.21 \pm 0.03$, occurs upon binding the first TNP-ATP molecule. Average binding of the first three molecules causes quenching of $\sim 0.55 \pm 0.03$, which corresponds to the first step in the binding isotherm; however, binding of the last three nucleotides gives the maximum saturation of six TNP-ATP molecules per DnaB hexamer and is accompanied by only an additional quenching of $\sim 0.21 \pm 0.05$. The dashed line represents the theoretical situation when the strict proportionality between the degree of nucleotide binding and the quenching of the DnaB protein fluorescence exists. It is clear that very pronounced nonlinearity exists between the extent of the protein fluorescence quenching and the degree of nucleotide binding, with the first three nucleotides binding with higher affinity and causing 70% of the total change of the protein fluorescence. The solid line in Figure

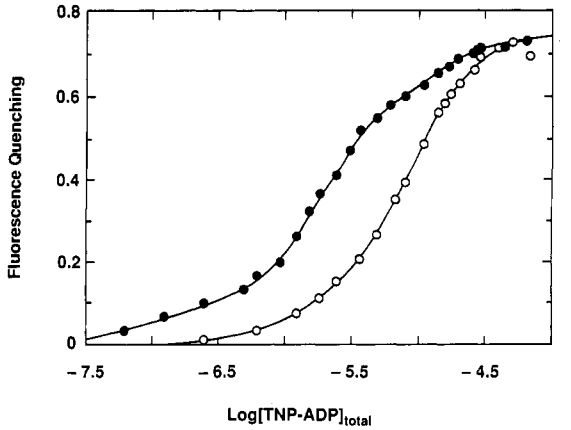

FIGURE 7: Fluorescence titration of the DnaB hexamer with TNP-ADP monitored by the quenching of the intrinsic protein fluorescence in buffer T2 + 20 mM NaCl (pH 8.1, 10 °C) at two different concentrations of the DnaB hexamer: (●) 5.62×10^{-7} M; (○) 3.51×10^{-6} M. Solid lines are added to separate the two data sets and have no theoretical basis.

6 is the nonlinear fit to a third degree polynomial defined by eq 5 with $a = 0.286$, $b = 0.0458$, and $c = 3.194 \times 10^{-3}$.

Determination of the stoichiometries of the binding of nucleoside diphosphate analog, TNP-ADP, to DnaB hexamer has been performed in an analogous way. Fluorescence titrations of the DnaB protein with TNP-ADP at two different protein concentrations are shown in Figure 7. At saturation the maximum quenching of DnaB protein fluorescence is 0.76 ± 0.05, which is identical to the value obtained for TNP-ATP binding. The biphasic character of the isotherms is more pronounced in the case of TNP-ADP binding, indicating a larger difference in affinity between high- and low-affinity binding steps. The analysis of these titration curves, as described under Materials and Methods, shows that six molecules of TNP-ADP are bound per DnaB hexamer at saturation. The dependence of the protein fluorescence quenching upon the number of TNP-ADP molecules bound to the DnaB hexamer is very similar, but not identical, to the experiments with TNP-ATP (Figure 6, closed circles). Average binding of the first three molecules causes $\sim 0.53 \pm 0.02$ quenching, while the next three nucleotides induce only $\sim 0.23 \pm 0.05$ quenching. The solid line is the nonlinear fit to a third degree polynomial defined by eq 5 with $a = 0.227$, $b = 0.0194$, and $c = 4.16 \times 10^{-4}$.

We also performed analogous fluorescence titrations and analysis for the binding of MANT-ADP to DnaB protein. As in the case of TNP derivatives, this nucleotide analog is also modified on the ribose (Figure 1; Hiratsuka, 1983). The binding isotherm of this analog is also biphasic (figures not shown). The thermodynamic binding parameters and fluorescence quenching constants for the binding of MANT-ADP to DnaB hexamer are included in Table I.

In order to test further the effect of the chemical modification on the binding of the nucleotide to DnaB, we performed fluorescence titrations with a different analog, εADP, which bears the modification on the adenine ring (see Figure 1). It should be noted that binding of εATP to DnaB protein could not be studied by steady-state fluorescence titrations because this analog is hydrolyzed by DnaB protein within the time comparable to the time scale of the titration experiments, even in the absence of ssDNA (Bujalowski and Klonowska, unpublished data). Fluorescence titrations of DnaB protein with εADP in buffer T2 + 20 mM NaCl, pH 8.1 (10 °C), at two different protein concentrations are shown in Figure 8. Binding of εADP to DnaB protein is accompanied by significant

Table I: Maximum Number of Bound Nucleotide Molecules, n, Intrinsic Binding Constant, K, Negative Cooperativity Parameter, σ, and the Maximum Fluorescence Quenching, Q_{max}, for TNP-ATP, TNP-ADP, TNP-AMP, MANT-ADP, and ϵADP Binding to DnaB Hexamer in Buffer T2 + 20 mM NaCl (pH 8.1, 10 °C)

binding parameter	TNP-ATP	TNP-ADP	TNP-AMP	ϵADP	MANT-ADP
n	6	6	ND[a]	6	6
K (M^{-1})[b]	$(5.9 \pm 1) \times 10^5$	$(2.15 \pm 0.4) \times 10^6$	$(1.52 \pm 0.3) \times 10^4$	$(7.2 \pm 1.5) \times 10^5$	$(1.2 \pm 0.2) \times 10^6$
σ	0.55 ± 0.05	0.31 ± 0.05	ND	0.33 ± 0.05	0.3 ± 0.05
Q_{max}	0.76 ± 0.05	0.76 ± 0.05	ND	0.53 ± 0.05	0.58 ± 0.05

[a] ND, not determined. [b] Intrinsic binding constant K and negative cooperativity parameter σ are based on the hexagon model: see eqs 6 and 9 in the text. The errors associated with the determination of K and σ are standard deviations obtained from 4–7 repeated titration experiments.

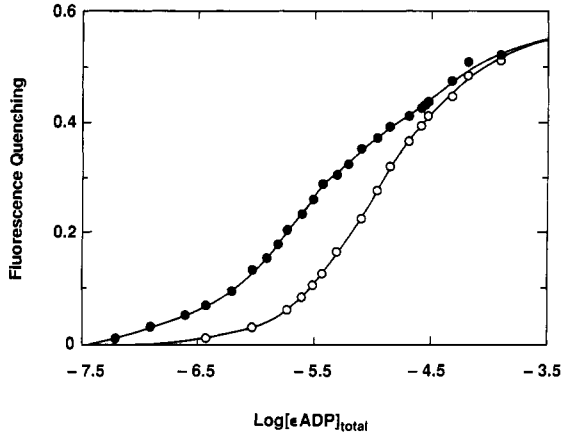

FIGURE 8: Fluorescence titration of the DnaB hexamer with ϵADP monitored by the quenching of the inrinsic protein fluorescence in buffer T2 + 20 mM NaCl (pH 8.1, 10 °C) at two different concentrations of the DnaB hexamer: (●) 5.61×10^{-7} M; (○) 3.51×10^{-6} M. Solid lines are added to separate the two data sets and have no theoretical bases.

quenching of the protein fluorescence. However, the extent of the quenching is smaller than in the case of TNP and MANT derivatives with the maximum quenching at saturation of 0.53 ± 0.05. The binding process is also biphasic, although the difference between the quenching of the protein fluorescence in two binding steps is much smaller. The first high-affinity and the second low-affinity phase are characterized by the quenching of 0.3 ± 0.03 and 0.23 ± 0.05, respectively. The absolute stoichiometry of the ϵADP–DnaB complex has been determined by the general analysis described under Materials and Methods. It shows that the DnaB hexamer binds a maximum of six molecules of ϵADP. The dependence of the protein fluorescence quenching upon the degree of binding is shown in Figure 6 (closed squares). The nonlinear least-squares fit gives $a = 0.141$, $b = 0.01302$, and $c = 6.9 \times 10^{-4}$.

Apparent Negative Cooperativity in Nucleotide Binding to DnaB Hexamer. A striking feature of the binding of nucleotide analogs to DnaB protein is the biphasic character of the binding process, which is indpendent of the type and location of the chemical modification on nucleotide. The biphasic character of the fluorescence binding isotherms results from the negative cooperative interactions among binding sites as well as nonlinear dependence of the protein fluorescence quenching as a function of the number of nucleotide molecules bound. For instance, in the case of TNP-ATP, TNP-ADP, and ϵADP binding to DnaB at 10 °C, the thermodynamic binding isotherm (the plot of the $\sum \nu_i$ versus free nucleotide concentration) shows a strong decrease in the affinity with the increase of the degree of binding (see Figure 10). However, this difference alone in the affinity is not large enough to produce visually significant separation in two binding phases. The biphasic character of the fluorescence binding isotherms obtained at 10 °C can only be seen due to the superposition

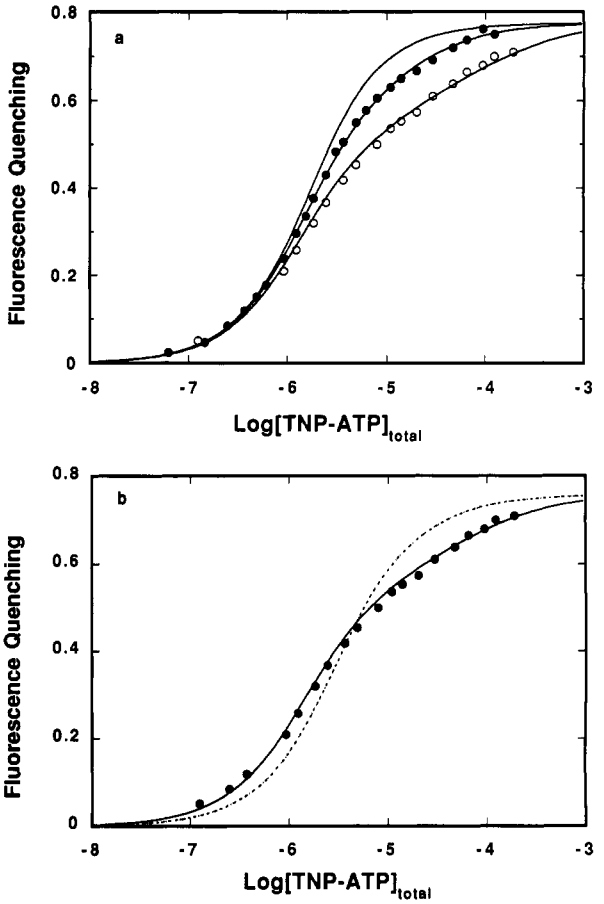

FIGURE 9: (a) Fluorescence titration of the DnaB hexamer with TNP-ATP monitored by the quenching of the intrinsic protein fluorescence in buffer T2 + 20 mM NaCl (pH 8.1) at two different temperatures: (●) 10 °C; (○) 28 °C. Solid lines are theoretical curves obtained using third degree polynomial representing exact relationship between the quenching of the protein fluorescence Q and the average degree of binding $\sum \nu_i$ (eq 5 with $a = 0.286$, $b = -0.0458$, $c = 3.194 \times 10^{-3}$) and interaction parameters obtained from nonlinear least-squares fit: $K = 5.9 \times 10^5$ M^{-1}, $\sigma = 0.53$ at 10 °C; $K = 5.5 \times 10^5$ M^{-1}, $\sigma = 0.25$ at 28 °C. The theoretical isotherm for the noncooperative binding ($\sigma = 1$), but with intrinsic affinity the same as at 10 °C ($K_{TNP\text{-}ATP} = 5.9 \sim 10^5$ M^{-1}) is also included (solid line without data points). The DnaB protein concentration is 5.50×10^{-7} M (hexamer). (b) Comparison between the computer fit of the experimental fluorescence isotherm of TNP-ATP binding to DnaB hexamer in buffer T2 + 20 mM NaCl (pH 8.1, 28 °C) (data from panel a) using the hexagon model, with the best fit of the same isotherm using a single class of six independent binding sites with intrinsic binding constant $K = 1.9 \times 10^5$ M^{-1} (dashed line).

of the difference in the affinity and the difference in the protein fluorescence quenching between the two binding steps.

The presence of two binding phases is more pronounced at higher temperatures. In Figure 9a the fluorescence titration of DnaB with TNP-ATP obtained at 10 °C is compared with the titration performed at 28 °C. The DnaB protein fully preserves its hexameric structure at this elevated temperature,

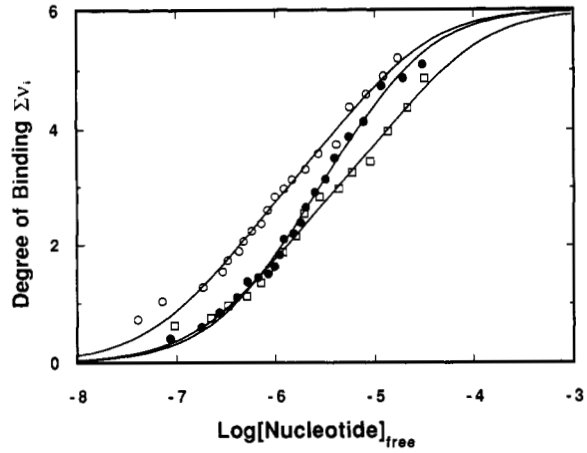

FIGURE 10: Average number of nucleotide molecules bound per DnaB hexamer as a function of the free concentration of nucleotide in buffer T2 + 20 mM NaCl (pH 8.1, 10 °C): (●) TNP-ATP; (○) TNP-ADP; (□) ϵADP. These isotherms have been constructed using the general method of analysis described under Material and Methods using eqs 3 and 4. The solid lines are nonlinear least-squares fits according to the hexagon model (eqs 6 and 9). The binding parameters are included in Table I.

as determined by sedimentation velocity experiments (Bujalowski and Klonowska, unpublished results). For comparison, a fluorescence binding isotherm for the noncooperative binding ($\sigma = 1$), but with intrinsic affinity the same as at 10 °C ($K_{TNP\text{-}ATP} = 5.9 \times 10^5$ M^{-1}), is included. Clearly, the experimental isotherms are composed of two binding steps. Because the functional dependence of the protein fluorescence quenching upon the number of nucleotide molecules bound is unchanged in the studied temperature range, the pronounced biphasic character of the binding isotherm at 28 °C results exclusively from an increased difference in the affinity between two binding steps at higher temperatures. Figure 9b shows the additional comparison between the best fit for the model of a single class of independent binding sites applied to the TNP-ATP binding to DnaB hexamer at 28 °C and the hexagon model with negative cooperative interactions among binding sites. It is evident that the model of a single class of independent binding sites, which does not include the decrease of the affinity with the increase of the degree of binding of the nucleotide on hexamer, does not describe the experimental isotherm. A similar increase of the separation of the two binding steps at higher temperatures has been observed for all studied nucleotide analogs (data not shown). Absolute stoichiometry determined by the general method shows that three molecules of nucleotide bind in the first step and the next three molecules bind in the second step.

The details of the two statistical thermodynamic models, namely, hexagon and octahedron, which describe the negative cooperative binding of six ligands to a macromolecules are given under Theory. The octahedron model does not predict the two-step behavior observed for TNP-ATP, TNP-ADP, and ϵADP binding to the DnaB hexamer (see Figures 5, 7, 8, and 9), even at very high negative cooperativity. In contrast, the hexagon model predicts the separation of the binding process into two steps at a high enough value of cooperativity parameter σ. Therefore, in order to obtain the intrinsic binding constant K and the negative cooperativity parameter σ, we have used the hexagon model.

The plot of the average degree of binding $\Sigma\nu_i$ of TNP-ATP, TNP-ADP, and ϵADP as a function of the logarithm of free nucleotide concentration in buffer T2 + 20 mM NaCl pH 8.1 (10 °C) is shown in Figure 10. The isotherms have been generated from an analysis of the two titration curves similar to those shown in Figures 5, 7, and 8 for TNP-ATP, TNP-ADP, and ϵADP, respectively, using eqs 3 and 4 (see Materials and Methods). The solid lines are nonlinear least square fits using eqs 6 and 8. The obtained intrinsic binding constants and cooperativity parameters are included in Table I. It is evident that TNP-ATP is more weakly bound to the DnaB hexamer than is TNP-ADP, with the intrinsic binding constant $K_{TNP\text{-}ATP} = (5.9 \pm 1) \times 10^5$ M^{-1} and $K_{TNP\text{-}ADP} = (2.1 \pm 0.4) \times 10^6$ M^{-1}, respectively. Binding of the TNP-ATP analog is also characterized by lower negative cooperativity than the binding of TNP-ADP (Table I). As a result, at a low concentration of nucleotides the DnaB hexamer preferentially binds TNP-ADP; however, at saturation the macroscopic affinity is very similar, and the two isotherms are very close to each other (Figure 10).

The negative cooperativity parameters σ are virtually the same for all studied nucleoside diphosphates, ϵADP, MANT-ADP, and TNP-ADP (Table I). Although the intrinsic affinities are different for these three ADP analogs, it is clear that the negative cooperativity is not affected by the type of chemical modification, whether the modification is on the ribose or adenine ring. These data suggest the important role of phosphate groups in inducing the negative cooperativity among binding sites.

Binding of adenosine monophosphate, TNP-AMP, to the DnaB hexamer is also accompanied by a strong quenching of the protein fluorescence. However, the affinity is very low and, even at the highest concentration of TNP-AMP applied (2×10^{-4} M), we reached only $Q_{obsd} = 0.5 \pm 0.03$ (data not shown). Higher concentrations of TNP-AMP necessary to saturate all binding sites of the DnaB hexamer require very large corrections for inner filter effect which would subject the isotherms to a significant error. Due to the low affinity, we could not apply the general method of analysis to determine the stoichiometry and cooperativity parameter σ for the monophosphate analog binding to the helicase. Even at very high protein concentrations, the fraction of TNP-AMP bound is always very small compared to the total nucleotide concentration. Nevertheless, the intrinsic binding constant $K_{TNP\text{-}AMP}$ and the quenching constant ΔQ_1 for the binding of the TNP-AMP to DnaB can be estimated by applying eq 13. This application is possible because, at any titration point in our experiments, $[TNP\text{-}AMP]_{total} \gg [DnaB]_{total}$; therefore, $[TNP\text{-}AMP]_{total} = [TNP\text{-}AMP]_{free}$ (L in eqs 11, 12, and 13). A plot of $1/Q_{obsd}$ versus $1/[TNP\text{-}AMP]_{total}$ is shown in Figure 11. This plot yields a straight line. From the slope and the intercept, we obtained $K_{TNP\text{-}AMP} = (1.52 \pm 0.3) \times 10^4$ M^{-1} and $\Delta Q_1 = 0.21 \pm 0.03$, respectively.

The intrinsic binding constant $K_{TNP\text{-}AMP}$ is, by a factor of ~40 and ~140, smaller than $K_{TNP\text{-}ATP}$ and $K_{TNP\text{-}ADP}$ (Table I). The extent of the dramatic drop in the affinity, as a result of the absence of the second phosphate group, is rather surprising when compared to the much smaller difference between $K_{TNP\text{-}ATP}$ and $K_{TNP\text{-}ADP}$. This result suggests a specific role of the second, and possibly third, phosphate group in the binding and recognition of nucleotide by DnaB helicase (see Discussion).

Higher affinity of TNP-ADP compared to TNP-ATP binding to DnaB hexamer determined in this work is in qualitative agreement with the data reported by Arai and Kornberg (1981c) who also found, using gel filtration and filter binding assay, that ATP binds weaker to DnaB than ADP. However, studying the nucleotide binding to DnaB protein by monitoring the fluorescence enhancement of the

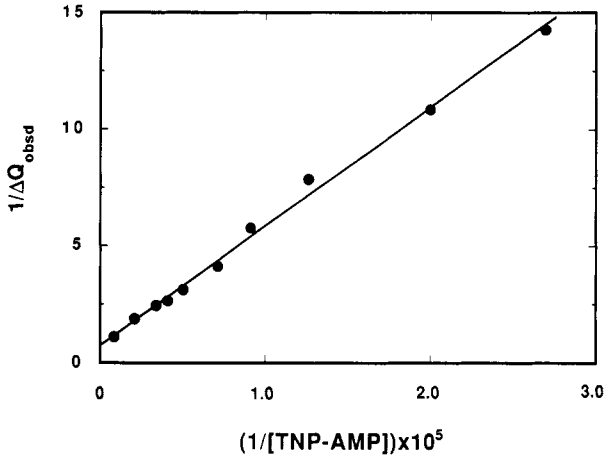

FIGURE 11: Dependence of the reciprocal of the DnaB protein fluorescence quenching $1/Q_{obsd}$ upon the reciprocal of the TNP-AMP concentration 1/[TNP-AMP] in buffer T2 + 20 mM NaCl (pH 8.1, 10 °C). The straight line is a least-squares fit based on eq 13 with $K_{TNP\text{-}AMP} = 1.52 \times 10^4$ M^{-1} and $\Delta Q_1 = 0.21 \pm 0.03$. DnaB protein concentration is 5.5×10^{-7} M (hexamer).

TNP analogs fluorescence, Biswas et al. (1886) reported higher affinity of the TNP-ATP than TNP-ADP to DnaB protein. These authors could not determine any binding affinity of TNP-AMP to DnaB protein. We believe that this discrepancy is partly due to assumptions used in the analysis of their data and to the limited concentration range of the TNP analogs studied (see Discussion). It should be pointed out that the experimental binding isotherms presented in Figure 10 are obtained independently of any assumptions.

Competition Effect of ADP on TNP-ATP and TNP-ADP Binding. Competition studies of the binding of nucleotide analogs with unmodified nucleotides are necessary to establish whether both ligands bind to the same binding sites. These studies may also serve to determine the binding parameters for the unmodified nucleotide whose binding is not accompanied by a change in the protein fluorescence significant enough to monitor the binding. ATP could not be used in the competition studies with its fluorescent analogs, because DnaB protein is efficiently hydrolyzing ATP even in the absence of ssDNA (Bujalowski and Klonowska, unpublished results). Therefore, ADP has been used in the competition experiments.

Several fluorescence titration curves of the DnaB protein with TNP-ATP in the presence of different concentrations of ADP in buffer T2 + 20 mM NaCl, pH 8.1 (10 °C), are shown in Figure 12a. The presence of ADP, even at as low a concentration as 2.4×10^{-6} M, significantly shifts the titration curve toward a higher TNP-ATP concentration range. This indicates strong competition between TNP-ATP and ADP, with ADP having the affinity for the binding sites similar to that of TNP-ATP. Also, the negative cooperativity of the binding of TNP-ATP to DnaB is lower in the presence of ADP. At high ADP concentration the binding of the ATP analog becomes independent and is characterized by $\sigma = 1 \pm 0.2$ (see Table II). Analogous competition experiments have been performed with TNP-ADP. As in the case of TNP-ATP, the titration curves are strongly shifted toward higher TNP-ADP concentrations with higher [ADP] (data not shown). Also, the negative cooperativity of the TNP-ADP binding is decreased in the presence of ADP; however, the binding does not become independent, even at the highest ADP concentration studied (see Table II).

The increase of the value of σ for TNP-ATP and TNP-ADP binding to DnaB protein, in the presence of ADP, can be interpreted as follows: the cooperativity parameter σ is

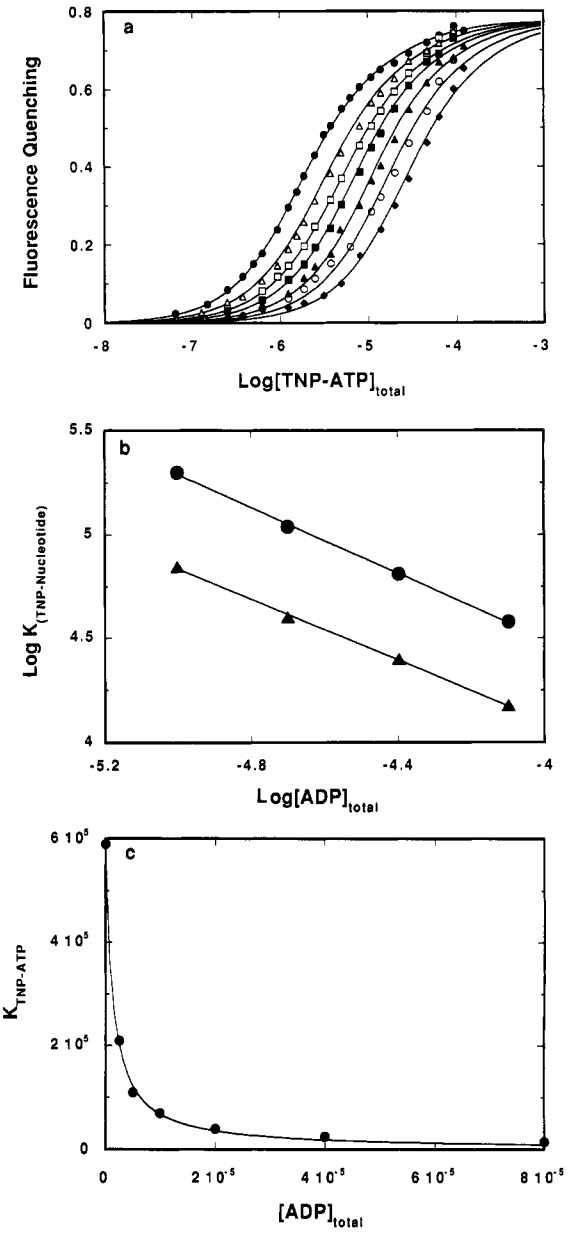

FIGURE 12: (a) Fluorescence titration of the DnaB hexamer with TNP-ATP monitored by the quenching of the intrinsic protein fluorescence in buffer T2 + 20 mM NaCl (pH 8.1, 10 °C) at different concentrations of ADP: (●) 0 M; (△) 2.5×10^{-6} M; (□) 5.0×10^{-6} M; (■) 1×10^{-5} M; (▲) 2×10^{-5} M; (○) 4×10^{-5} M; (◆) 8×10^{-5} M. The solid lines are theoretical curves based on hexagon model using the nonlinear least-squares fit values of K and σ included in Table II. The DnaB protein concentration is 5.40×10^{-7} M (Hexamer); (b) Dependence of the logarithm of the intrinsic binding constants, $K_{TNP\text{-}ATP}$ and $K_{TNP\text{-}ADP}$, upon the logarithm of ADP concentration determined from titrations shown in figure 10a: (▲) TNP-ATP; (●) TNP-ADP. (c) Dependence of intrinsic binding constant $K_{TNP\text{-}ATP}$ upon ADP concentration in buffer T2 + 20 mM NaCl (pH 8.1, 10 °C). The solid line is the theoretical curve generated using the value of $K_{ADP} = (8.1 \pm 1.5) \times 10^5$ M^{-1} obtained from a nonlinear least-squares fit according to eq 15.

formally the equilibrium constant characterizing the transfer process 01 ± 01 ↔ 11 + 00, where 0 is the empty and 1 is the bound site, respectively (Hill, 1985). In the case of negative cooperativity, the value of $\sigma < 1$ indicates that the transfer of the ligand molecules (TNP-ATP or TNP-ADP) to neighboring sites is accompanied by an increase in the free energy of the system. In the presence of the saturating concentration of the second ligand (ADP), this equilibrium can formally be written as X1 + X1 ↔ 11 + XX, where X is the binding site

Table II: Intrinsic Binding Constant K and Negative Cooperativity Parameter σ for TNP-ATP and TNP-ADP Binding to DnaB Hexamer in Buffer T2 + 20 mM NaCl (pH 8.1, 10 °C) at Different ADP Concentrations

[ADP] (M)	TNP-ATP		TNP-ADP	
	K (M^{-1})[a]	σ	K (M^{-1})	σ
0	$(5.9 \pm 1.5) \times 10^5$	0.53 ± 0.05	$(2.1 \pm 0.4) \times 10^6$	0.31 ± 0.05
2.5×10^{-6}	$(2.1 \pm 0.4) \times 10^5$	0.71 ± 0.05		
5.0×10^{-6}	$(1.1 \pm 0.3) \times 10^5$	0.80 ± 0.05	$(3.3 \pm 0.6) \times 10^5$	0.50 ± 0.05
1.0×10^{-5}	$(7.0 \pm 1.5) \times 10^4$	0.90 ± 0.10	$(2.0 \pm 0.5) \times 10^5$	0.60 ± 0.06
2.0×10^{-5}	$(4.0 \pm 1.0) \times 10^4$	1.0 ± 0.15	$(1.1 \pm 0.2) \times 10^5$	0.66 ± 0.05
4.0×10^{-5}	$(2.5 \pm 0.5) \times 10^4$	1.0 ± 0.20	$(6.5 \pm 1.2) \times 10^4$	0.70 ± 0.15
8.0×10^{-5}	$(1.5 \pm 0.6) \times 10^4$	1.0 ± 0.20	$(3.8 \pm 0.7) \times 10^4$	0.90 ± 0.15

[a] Intrinsic binding constant K and negative cooperativity parameter σ are based on the hexagon model: see eqs 6 and 9 in the text. The errors associated with the determination of K and σ are standard deviations obtained from 4–7 repeated titration experiments.

saturated with ADP. The increase of the σ value for TNP-ATP and TNP-ADP binding to DnaB hexamer in the presence of ADP suggests that there are negative cooperative interactions in the X1 complex strong enough to make the transfer process energetically less unfavorable.

At the concentrations of ADP used in these experiments, $[ADP]_{total} \gg [DnaB]_{total}$; therefore, $[ADP]_{total}$ is practically equal to $[ADP]_{free}$. Thus, we were able to estimate the number of ADP molecules, m, competing with nucleotide analogs for the binding site on DnaB hexamers using Wyman's linkage relation (Wyman, 1964; Wyman & Gill, 1990):

$$\partial \log K_{TNP\text{-}N}/\partial \log [ADP]_{free} = -m \qquad (14)$$

where $K_{TNP\text{-}N}$ is the intrinsic binding constant of the nucleotide analog. The value of m will be closer to the number of competing ADP molecules at higher ADP concentrations, where the binding sites are saturated. The dependence of the logarithm of the intrinsic binding constant $K_{TNP\text{-}ATP}$ and $K_{TNP\text{-}ADP}$ upon the logarithm of the free ADP concentration is shown in Figure 12b. The slopes $\partial \log K_{TNP\text{-}ADP}/\partial \log [ADP]_{free} = 0.8 \pm 0.1$ and $\partial \log K_{TNP\text{-}ATP}/\partial \log [ADP]_{free} = 0.75 \pm 0.1$, respectively. These values are close to but slightly lower than 1, which reflects the fact that even at the highest concentrations of ADP applied in our competition experiments (8×10^{-5} M) DnaB is not 100% saturated with ADP. Thus binding of TNP nucleotide analogs releases one ADP molecule from the binding site on DnaB protein. This result also indicates that ADP competes for all six binding sites with TNP-ATP and TNP-ADP.

The approximate estimation of the ADP binding constant to its binding site on DnaB hexamer can be obtained using the relationship for the intrinsic binding constant of the TNP-ATP, $K_{TNP\text{-}ATP}$, competing for the same discrete binding site on a macromolecule with ADP and defined by the thermodynamic relation (Hill, 1985)

$$K_{TNP\text{-}ATP} = K(_{TNP\text{-}ATP})_o/(1 + K_{ADP}[ADP]_{free}) \qquad (15)$$

where $K(_{TNP\text{-}ATP})_o$ is the intrinsic binding constant of the TNP-ATP in the absence of ADP, and K_{ADP} is the binding constant of ADP. Therefore, the intrinsic binding constant of the nucleotide analog should be a simple hyperbolic function of $[ADP]_{free}$. The dependence of the intrinsic binding constant of TNP-ATP upon [ADP] is shown in Figure 12c. The solid line is the computer fit according to eq 15, with a single parameter, $K_{ADP} = (8.1 \pm 1.5) \times 10^5$ M^{-1}. Analogous competition experiments and analysis of the dependence of intrinsic binding constants for TNP-ADP and ϵADP, as a function of [ADP], provided $K_{ADP} = (1 \pm 0.2) \times 10^6$ M^{-1} and $(8.5 \pm 1.7) \times 10^5$ M^{-1}, respectively (plots not shown). As expected, these values are very close because eq 15 is a general thermodynamic relation and is independent of the type of competing ligands as long as the cooperative interactions between them are very similar, as in the case of ADP analogs.

DISCUSSION

Binding and/or hydrolysis of ribonucleotide triphosphates (rNTP's) is crucial in regulating the functions of DnaB protein. Although the enzyme can bind and hydrolyze all four rNTP's with similar affinity and efficiency, ATP plays a particular role being specifically required in some functions, e.g., formation of the specific DnaB–ssDNA structures as a recognition site for primase (Arai & Kornberg, 1981b; Kaguni et al., 1982).

In this report, we systematically probed the interactions of nucleotides with DnaB protein, using different fluorescent nucleotide analogs, differing by the type and the location of the modifying group. In the case of TNP-ATP, TNP-ADP, TNP-AMP, and MANT-ADP, the fluorescent groups, trinitrophenyl (TNP) and methylantraniloyl (MANT), are attached to the ribose 2′ and/or 3′ oxygens, whereas in ϵADP the modification is located on the adenine (Figure 1).[2]

Fluorescent analogs appear to be extremely useful in studying the equilibrium and kinetic properties of different ATPases (Moczydlowski & Fortes, 1981a,b; Leonard, 1984 and references therein). Partly, this application results from the fact that binding of ATP or ADP very often does not cause large enough changes in the physicochemical properties of these enzymes, making quantitative analysis very difficult. A common approach in studying these interactions has been to examine the fluorescent properties of the nucleotide analogs. However, in the case of TNP, MANT, and etheno derivatives, there is a significant overlap of the protein tryptophan fluorescence emission spectrum and absorption spectrum of the analogs. This indicates a possible energy transfer from tryptophan to nucleotide which could result in quenching of the protein fluorescence and, in turn, be used to monitor the binding. As we have shown in this work, binding of TNP, MANT, and etheno analogs to DnaB hexamer is indeed accompanied by strong quenching of the protein fluorescence. Although not all observed quenching may result from fluorescence energy transfer, independent measurements of the sensitized fluorescence of nucleotide analogs shows strong fluorescence energy transfer from protein tryptophans to nucleotides, indicating close proximity between the nucleotide binding sites and the tryptophans (Bujalowski and Klonowska, manuscript in preparation). It is possible that similar strong quenching of the protein fluorescence upon TNP, MANT, or etheno derivatives binding will be observed in the case of other helicases, provided that the structure of the nucleotide binding sites are similar in these functionally homologous enzymes.

The general method of analysis applied in this work allows absolute stoichiometries and binding parameters to be obtained without any assumption about the relationship between observed optical parameters and the degree of binding. Using this rigorous method, we determined that at saturation, the DnaB protein hexamer binds six molecules of each nucleotide studied and that there is a strong difference in the affinity among binding sites. There is a nonlinear dependence of the extent of the protein fluorescence quenching and the degree

[2] On the basis of chemical studies, MANT-ATP and MANT-ADP were originally postulated to exist solely as 3′ isomers (Hiratsuka et al., 1983). Recent NMR studies indicate that MANT-ATP and MANT-ADP may exist as a mixture of 2′ and 3′ isomers, with the 3′ isomer being significantly predominant (Cremo et al., 1990).

of binding. In particular, TNP derivatives which exhibit a 70% of the total fluorescence change reached at only 50% of the total protein saturation with the ligand.

In cases where all molecular fluorescence parameters can be determined (Bujalowski & Lohman, 1989a,b), the analytical equation, analogous to eq 11, can be obtained relating the observed quenching to the molecular fluorescence and to thermodynamic binding parameters. However, this approach is inapplicable for DnaB–nucleotide systems due to the large number of possible molecular fluorescence parameters characteristic for each possible configuration of the protein with different numbers of nucleotide molecules bound. These parameters cannot be obtained independently. The approach we used in this work has allowed us to overcome this problem by introducing an empirical function, which exactly relates the observed fluorescence quenching to the absolute average degree of binding $\sum \nu_i$. This empirical function was then applied in all simulation and fitting procedures. Another approach would be to apply a complex multiparameter computer fitting. However, this is limited to rather simple cases with relatively small numbers of parameters (Bujalowski & Porschke, 1984, 1988a,b).

We have shown that the macroscopic affinity of the nucleotide binding to DnaB is biphasic, i.e., the first three nucleotide molecules bind with higher affinity than the next three molecules, particularly at higher temperatures (Figure 9). This behavior could be interpreted as the existence of two different, independent classes of binding sites on the DnaB hexamer. Such an interpretation cannot be ruled out on the basis of equilibrium binding experiments alone. We favor the interpretation that the biphasic character of the binding process reflects the existence of negative cooperativity between neighboring sites on the hexamer for the following reasons. The DnaB protein is composed of six chemically identical subunits. Most likely, all subunits in the free protein are initially equivalent; thus, the negative cooperativity would result from conformational changes induced by ligand binding. The dependence of the protein fluorescence quenching upon the degree of binding of nucleotides, particularly in the case of TNP derivatives, indicates the sequential nature of the ligand-induced conformational changes (Figures 5–9). Binding of the first nucleotide molecule to the hexamer induces the largest conformational change, whereas subsequent nucleotide molecules contribute progressively less to the total fluorescence quenching. Thus, nonequivalent quenching also suggests the existence of the interactions among binding sites and ligand-induced conformational changes as a dominant factor in negative cooperativity. Moreover, different nucleoside diphosphate analogs, TNP-ADP, MANT-ADP, and ϵADP, have different intrinsic affinities but virtually the same negative cooperativity factor σ (Table I). Such a situation would require that, in the case of two independent classes of binding sites, two corresponding intrinsic binding constants change with the type and location of chemical modification, but the ratio of the intrinsic binding constants is exactly the same for all three nucleotide analogs studied. This is a possible, but rather unlikely, situation if the sites are initially physically different. However, it should be pointed out that there may be two different classes of nucleotide binding sites on DnaB hexamer with additional negative cooperative interactions among them.

Two simple sequential binding models can incorporate negative cooperativity among ligand binding sites on the hexamer, namely, the hexagon and octahedron models. Although both models use only two parameters, the intrinsic binding constant K and cooperativity parameter σ, only the hexagon model can predict, for values of $\sigma < 1$, the biphasic binding isotherm, in which three molecules of nucleotides bind in each binding phase. From a thermodynamic point of view, the excellent description of the nucleotide binding to the DnaB protein hexamer by the hexagon model indicates that cooperative interactions are limited to the nearest neighbor sites or are predominant between nearest neighbor sites (Hill, 1985). Only at this low density of cooperative interactions will there be a configuration of the hexamer, with three molecules of the nucleotide bound, which has much lower free energy than other configurations with three nucleotides bound. In the alternative octahedron model, the density of cooperative interactions is much higher, and there are no configurations with three bound nucleotide molecules which can have significantly lower free energy than the others. As a result, the octahedron model does not predict the separation of the binding process into two steps with an equal number of ligand molecules bound in each step, for $\sigma \ll 1$. Therefore, the binding of nucleotides to DnaB hexamer cannot be described by the octahedron model (Figure 3b).

As we pointed out, the nucleotide analogs of ADP studied in this work differ by the type and the location of the modifying group and have different intrinsic affinities, but they have a very similar negative cooperativity factor σ. Moreover, ϵATP is hydrolyzed by DnaB protein with an efficiency similar to that of ATP hydrolysis (Bujalowski and Klonowska, unpublished data). The intrinsic affinity of ϵADP is, within experimental accuracy, the same as that of unmodified ADP, indicating that this modification does not affect either catalytic or binding process to a significant degree. Thus, these results indicate that negative cooperativity does not result from the presence of a particular chemical modification of the analog but that it is an *intrinsic property* of the DnaB hexamer.

It is interesting that intrinsic affinity of TNP-ADP is higher by a factor of $\sim$3.6 than that of TNP-ATP but is $\sim$140-fold higher than that of TNP-AMP (see Table I). Thus, the presence of the second phosphate group seems to be crucial for the binding and recognition of the nucleotide by the DnaB helicase. The mechanism of this dramatic enhancement of the affinity is still unknown. It is possible that the intrinsic binding of ATP and ADP to the DnaB helicase is, at least, a two-step process with the second step induced only by the interactions of the second phosphate group in the active site. At this point, it should be noted that binding of TNP-ATP is characterized by a weaker negative cooperativity than TNP-ADP binding. On the other hand, ϵADP binds with the same negative cooperativity but more weakly than either TNP-ADP or MANT-ADP. This result suggests that the adenine ring does not affect the negative cooperativity and that the differences in the interactions in the adenine binding site between TNP-ADP, MANT-ADP, and ϵADP are not transmitted to the ribose–phosphate region. This would be consistent with the fact that DnaB can hydrolyze different NTP's in the presence of ssDNA with similar efficiency and with only slight preference for ATP (Arai & Kornberg, 1981b). Thus, the negative cooperative interactions appear to be specifically modulated by the presence of a second, and possibly a third, phosphate group.

There are only two previous quantitative studies of ATP binding to DnaB protein (Arai & Kornberg, 1981b; Biswas et al., 1986). Using filter binding and gel filtration techniques, Arai and Kornberg found that at 0 °C six molecules of ATP or ADP bind to the DnaB hexamer at maximum saturation. This is in agreement with the stoichiometries obtained in this

work, although these authors did not observe any negative cooperativity in nucleotide binding to the DnaB protein. However, it should be noted that binding isotherms measured at two temperatures, 10 and 28 °C, show that negative cooperative interactions among nucleotide binding sites on DnaB hexamer are significantly weaker at lower temperatur (see Figure 9), whereas intrinsic affinity is affected very litt in the studied temperature range. We also measured th binding of the TNP-ATP at 0 °C to obtain direct comparison with Arai and Kornberg results (plots not shown). Within the accuracy of the binding experiments, there is no detectable negative cooperativity in TNP-ATP binding to DnaB hexamer at this temperature ($K_{TNP\text{-}ATP} = 7.3 \times 10^5$ M^{-1}, $\sigma = 1 \pm 0.2$). Therefore, it is possible that at 0 °C the negative cooperativity among nucleotide binding sites saturated with unr ified nucleotides is also very weak and undetectable. l the limited number of experimental points, slight negative cooperativity would be difficult to detect from Scatchard plots in the Arai and Kornberg work. Systematic studies of the temperature's effect on nucleotide binding to DnaB are now being undertaken in our laboratory.

Using fluorescence titration techniques and monitoring the enhancement of TNP-ATP and TNP-ADP fluorescence upon binding to DnaB, Biswas et al. (1986) obtained that only three molecules of modified nucleotides bind to the DnaB hexamer. These estimates are different by a factor of 2 from the data we report here. The authors attributed the low stoichiometries to the possible effect of the "bulky" TNP group, which could only be accommodated in three binding sites. However, studying the binding of the TNP-ATP, TNP-ADP, MANT-ADP, and εADP to DnaB protein, by monitoring the quenching of the protein fluorescence upon nucleotide binding, we found that the DnaB hexamer binds six molecules of nucleotide analogs. It should be pointed out that Biswas et al. (1986) performed their titrations at very limited concentration ranges, only up to $\sim 10^{-5}$ M of total nucleotide concentration. Unfortunately, because the authors did not include temperature in their fluorescence titration protocols, we could not estimate negative cooperativity in their experiments. However, if the temperature was higher than 10 °C, the separation of the two binding phases could be large enough so that only the binding of three nucleotides could be detected in the limited concentration ranges studied by the authors. Using our binding parameters (K and σ) determined at 10 and 28 °C, we calculated the degree of binding of TNP-ATP and TNP-ADP at the highest concentration ($\sim 10^{-5}$ M) of these nucleotides used by Biswas et al. (1986). We obtained that, in this limited concentration range at 10 or 28 °C, only 3–3.5 nucleotide molecules are bound per DnaB hexamer (see Figure 10), which is similar to the low stoichiometry of the complexes determined by these authors. Moreover, the analysis of fluorescence titration experiments performed by Biswas et al. (1986) was based on the assumption that measured fractional changes in the signal from the ligand (TNP derivatives) equals the fractional ligand saturation. As we pointed out (see Materials and Methods), this assumption may not be correct and may lead to severe underestimations of the ligand–macromolecule stoichiometries if there is a significant heterogeneity in the ligand fluorescence enhancement at a different degree of binding.

Biswas et al. (1986) determined also that TNP-ADP binds more weakly ($K_D = 2.8 \times 10^{-6}$ M) than TNP-ATP ($K_D = 0.87 \times 10^{-6}$ M) in contradiction to the fact that the midpoint of their fluuorescence titration with TNP-ATP is located at a higher nucleotide concentration (1 μM) compared to TNP-ADP (0.75 μM). This result indicates that TNP-ATP has a rather lower affinity than TNP-ADP, which is in agreement with our data. As we discussed above, we believe that this discrepancy in their own data lies in part with the method of analysis of the binding isotherms applied by these authors.

The importance of the negative cooperativity in nucleotide binding to the DnaB protein may lie in the fact that DnaB is a multisubunit protein involved in many processes *in vivo* in which nucleotide binding plays a regulatory role (Arai & Kornberg, 1981a–c; Lebowitz & McMacken, 1986). It has been proposed that some of these processes are controlled positively but some are controlled negatively by ATP or ADP binding. For instance, there are indications that the affinity of the protein for ssDNA is strongly increased in the presence of ATP analogs, but in the presence of ADP this affinity is diminished (Arai & Kornberg, 1981b). Formation of the specific DnaB–ssDNA complex recognized by primase requires ATP as a positive effector but is inhibited by ADP (Arai & Kornberg, 1981b). Also, the regulatory role of ATP in DnaB–DnaC complex formation has been implicated. The stable complex is formed in the presence of ATP but not ADP (Wahle et al., 1989a,b). It has also been suggested that part of the ATP molecules are removed from DnaB protein upon complex formation with DnaC protein (Biswas et al., 1986). Negative cooperativity introduces functional differentiation among otherwise identical DnaB protein subunits. With the negative cooperative interactions limited to the neighboring binding sites, the hexamer forms functionally a dimer of trimers. This functional asymmetry will enable the protein to hydrolyze ATP to ADP by one set of subunits, but the enzyme will still preserve strong affinity for ssDNA and DnaC protein by the other set of subunits not bound with ADP. This may play an important role in the priming reaction at the origin of the *E. coli* chromosome (*oriC*) where the complex DnaB–DnaC is absolutely required (Wahle et al., 1989a,b). The same mechanism may also be involved in the helicase activity of the enzyme in the replication fork where, during the unwinding of the duplex DNA with concomitant hydrolysis of ATP, the cycling of the DnaB binding between ssDNA and dsDNA conformation occurs (Lebowitz & McMacken, 1986; Baker et al., 1987). At this point, it should be noted that the optimal concentration of ATP for DnaB-catalyzed unwinding of duplex DNA is ~2 orders of magnitude higher than the K_m values for ATP in the presence of ssDNA (Lebowitz & McMacken, 1986). It is therefore possible that this difference reflects functional heterogeneity among different sets of binding sites resulting from negative cooperativity among them.

The equilibrium binding data and the analysis presented in this work indicate a complex mechanism of the nucleotide binding to DnaB helicase and suggest sophisticated interplay between the nucleotide and the amino acid residues in the active site. The resulting differences in the relative affinities and negative cooperativities between ATP and ADP may play important roles in the free energy transduction by DnaB protein, when the enzyme functions on nucleic acid.

ACKNOWLEDGMENT

We especially thank Dr. Tomasz Heyduk for the many helpful discussions and commments on the manuscript. We thank Drs. Edmund W. Czerwinski, James C. Lee, and Alexander Kurosky for their careful reading and comments on the manuscript. We also thank Dr. Robert MacGregor for excellent professional help in growing bacterial cell cultures.

REFERENCES

Allen, G. C., & Kornberg, A. (1991) *J. Biol. Chem. 266*, 22096–22101.

Arai, K., & Kornberg, A. (1981a) *J. Biol. Chem. 256*, 5253–5259.

Arai, K., & Kornberg, A. (1981b) *J. Biol. Chem. 256*, 5260–5266.

Arai, K., & Kornberg, A. (1981c) *J. Biol. Chem. 256*, 5267–5272.

Arai, K., Yasuda, S., & Kornberg, A. (1981a) *J. Biol. Chem. 256*, 5247–5252.

Arai, K., Low, R. L., & Kornberg, A. (1981b) *Proc. Natl. Acad. Sci. U.S.A. 78*, 707–711.

Arai, K., Low, R., Kobori, J., Shlomai, J., & Kornberg, A. (1981c) *J. Biol. Chem. 256*, 5273–5280.

Baker, T. A., Funnell, B. E., & Kornberg, A. (1987) *J. Biol. Chem. 262*, 6877–6885.

Biswas, E. E., Biswas, B., & Bishop, J. E. (1986) *Biochemistry 25*, 7368–7374.

Biswas, S. B., & Biswas, E. E. (1987) *J. Biol. Chem. 262*, 7831–7838.

Bruist, M. F., & Hammes, G. G. (1982) *Biochemistry 21*, 3370–3377.

Bujalowski, W., & Porschke, D. (1984) *Nucleic Acid Res. 12*, 7549–7563.

Bujalowski, W., & Lohman, T. M. (1987) *Biochemistry 26*, 3099–3106.

Bujalowski, W., & Porschke, D. (1988a) *Biophys. Chem. 30*, 151–157.

Bujalowski, W., & Porschke, D. (1988b) *Z. Naturforsch. 43c*, 91–98.

Bujalowski, W., & Lohman, T. M. (1989a) *J. Mol. Biol. 207*, 249–269.

Bujalowski, W., & Lohman, T. M. (1989b) *J. Mol. Biol. 207*, 268–288.

Cheung, H. C., Gonsoulin, F., & Garland, F. (1985) *Biochim. Biophys. Acta 832*, 52–62.

Cremo, C. R., Neuron, J. M., & Yount, R. G. (1990) *Biochemistry 29*, 3309–3319.

Gill, S. C., & von Hippel, P. H. (1989) *Anal. Biochem. 182*, 319–326.

Halfman, C. J., & Nishida, T. (1972) *Biochemistry 11*, 3493–3498.

Hill, T. L. (1985) *Cooperativity Theory in Biochemistry*, Springer-Verlag, New York.

Hiratsuka, T. (1983) *Biochim. Biophys. Acta 742*, 496–508.

Hiratsuka, T., & Uchida, K. (1973) *Biochim. Biophys. Acta 320*, 635–647.

Kaguni, J. M., Fuller, R. S., & Kornberg, A. (1982) *Nature 296*, 623–626.

Kobori, J. A., & Kornberg, A. (1982a) *J. Biol. Chem. 257*, 13757–13762.

Kobori, J. A., & Kornberg, A. (1982b) *J. Biol. Chem. 257*, 13763–13769.

Kobori, J. A., & Kornberg, A. (1982c) *J. Biol. Chem. 257*, 13770–13775.

Kornberg, A., & Baker, T. A. (1992) *DNA Replication* Freeman, San Francisco, CA.

Lakowicz, J. R. (1983) *Principle of Fluorescence Spectroscopy*, Chapter 10, Plenum Press, New York.

Lanka, E., Geschke, B., & Schuster, H. (1978) *Proc. Natl. Acad. Sci. U.S.A. 75*, 799–803.

LeBowitz, J. H., & McMacken, R. (1986) *J. Biol. Chem. 261*, 4738–4748.

Lee, M. S., & Marians, K. J. (1989) *J. Biol. Chem. 264*, 14531–14542.

Lohman, T. M., & Bujalowski, W. (1991) *Methods Enzymol. 208*, 258–290.

Leonard, N. J. (1984) *Crit. Rev. Biochem. 15*, 125–199.

Mallory, J. B., Alfano, C., & McMacken, R. (1990) *J. Biol. Chem. 265*, 13297–13307.

Matson, S. W., & Kaiser-Rogers, K. A. (1990) *Annu. Rev. Biochem. 59*, 289–329.

Moczydlowski, E. G., & Fortes, P. A. G. (1981a), *J. Biol. Chem. 256*, 2346–2356.

Moczydlowski, E. G., & Fortes, P. A. G. (1981b) *J. Biol. Chem. 256*, 2357–2366.

McMacken, R., Ueda, K., & Kornberg, A. (1977) *J. Biol. Chem. 253*, 3313–3319.

Nakayama, N., Arai, N., Kaziro, Y., & Arai, K. (1984a) *J. Biol. Chem. 259*, 88–96.

Nakayama, N., Arai, N., Bond, M. W., Kaziro, Y., & Arai, K. (1984b) *J. Biol. Chem. 259*, 97–101.

Parker, C. A. (1968) *Photoluminescence of Solutions* Elsevier Publishing Co., Amsterdam.

Perkins, W. J., Wells, J. A., & Yount, R. G. (1984) *Biochemistry 23*, 3994–4002.

Reha-Krantz, L. J., & Hurwitz, J. (1978a) *J. Biol. Chem. 253*, 4043–4050.

Reha-Krantz, L. J., & Hurwitz, J. (1978b) *J. Biol. Chem. 253*, 4051–4057.

Schekman, R., Weiner, A., & Kornberg, A. (1974) *Science 186*, 987–993.

Schekman, R., Weiner, J. H., Weiner, A., & Kornberg, A. (1975) *J. Biol. Chem. 250*, 5859–5865.

Secrist, J. A., Bario, J. R., Leonard, N. J., & Weber, G. (1972) *Biochemistry 11*, 3499–3506.

Ueda, K., McMacken, R., & Kornberg, A. (1978) *J. Biol. Chem. 253*, 261–269.

Van der Ende, A., Baker, T., Ogawa, T., & Kornberg, A. (1985) *Proc. Natal. Acad. Sci. U.S.A. 82*, 3954–3954.

Wahle, E., Lasken, R. S., & Kornberg, A. (1989a) *J. Biol. Chem. 264*, 2463–2468.

Wahle, E., Lasken, R. S., & Kornberg, A. (1989b) *J. Biol. Chem. 264*, 2469–2475.

Wickner, S. H. (1978) *Cold Spring Harbor Symp. Quant. Biol. 43*, 303–310.

Wickner, S., Wright, M., & Hurwitz, J. (1973) *Proc. Natl. Acad. Sci. U.S.A. 71*, 783–787.

Wyman, J. (1964) *Adv. Protein Chem. 19*, 223–286.

Wyman, J., & Gill, S. J. (1990) *Binding and Linkage. Functional Chemistry of Biological Macromolecules*, University Science Books, Mill Valley, CA.